

# **Analysis of dielectric charging assessment through up-state capacitance-voltage characteristic in MEMS capacitive switches**

M. KOUTSOURELI\*, D. BIRMPILIOTIS, L. MICHALAS and  
G. PAPAIOANNOU

Physics Department, University of Athens, 15784 Panepistimioupolis, Athens,  
Greece, Phone: +30 2107276722,

\*Email: mkoutsourel@phys.uoa.gr.

**Abstract.** The present paper aims to provide a better approach on the analysis of pull-up capacitance-voltage characteristic of MEMS capacitive switches by introducing an analytical model that takes into account the case of a real device, where the charge is not uniformly distributed at the surface of the dielectric film and the switch armatures are not parallel. The proposed model allows the use of capacitance-voltage characteristic's derivative, which slope is directly related to the device mechanical characteristics and the stress induced during charging. The application of the model on a MEMS switch with a parabolic up-state capacitance-voltage characteristic during charging and discharging processes allows the draw of conclusions on the charging and the mechanical performance of the devices.

## **1. Introduction**

Capacitive RF MEMS switches are very promising devices for RF applications due to their small size, weight and possibility to be integrated in ICs. Despite these advantages reliability problems still hinder their commercialization, the most important being the effect of the dielectric charging that causes erratic device behavior [1].

The dielectric charging of the insulating film in capacitive MEMS switches has been intensively investigated by employing various assessment methods in both MEMS and MIM (Metal-Insulator-Metal) devices [2,3,4]. The lifetime of capacitive switches has been determined by monitoring the number of cycles to stiction or the shift of pull-in voltage under different actuation voltage profiles, device temperatures [1,5,6,7] and ambient conditions [8]. Meanwhile, a different approach has been proposed J. Wibbeler *et al.* [9] for the calculation of dielectric

film's surface net charge in capacitive MEMS switches with parallel armatures. The latter approach has been adopted in [10, 11, 12, 13] and [14] where a fast algorithm was derived for the calculation of the dielectric film charge density. The method in [9] was based on the recording of the up-state capacitance-voltage (C-V) characteristic, determining the bias for the minimum capacitance, calculating the net surface charge and monitoring the evolution of the net charge during charging or discharging processes. The advantage of this method arises from the fact that it is not affected by the moving armature creep, which decreases the device pull-in voltage and therefore does not allow the accurate calculation of net charge from the shift of pull-in or pull-out voltages  $X$ .

Rottenberg *et al.* [15] has proposed a more realistic model for the case of switches with non-parallel armatures and distributed charge across the surface of the dielectric film. Assuming small capacitance variance, the model was applied to the calculation of the long-term discharge current through the dielectric film [16] and to study the contacted and induced charging as well as the discharging current flowing through the dielectric film in capacitive switches during up-state [17]. Beyond these the observed broadening or narrowing of the up-state C-V characteristic and its continuous variation during charging or discharging has not received the appropriate consideration and obviously it has not been exploited for extraction of additional information related to device degradation.

The aim of the present paper is to derive analytical equations for the up-state capacitance-voltage characteristic of real MEMS capacitive switches with non-planar electrodes and distributed trapped charges, which will improve the characterization methodology and allow the obtaining of a better insight on the dielectric charging assessment. Devices with symmetric up-state C-V characteristics, for small displacement from equilibrium state, illustrate the importance of the proposed model and the related methodology. The experimental results are used to draw conclusion on the device electrical and mechanical performance.

## 2. Theoretical Model

In order to investigate dielectric charging phenomena in the present work we adopted the device model proposed in [15], presented in Fig.1, which includes a fixed non-flat metal plate of area  $A$  covered with a dielectric film of uniform thickness and a dielectric constant  $\epsilon_r$ . Above it a rigid but non-flat moveable metal plate is fastened with a linear spring  $k$  to a fixed wall above the dielectric layer at a rest position  $d_0(x,y)$ . When a DC voltage  $V$  is applied between the two plates, the moving plate is displaced by  $\Delta$  from its rest position to a new position  $d(x,y)$ . In such a device the movable electrode displacement ( $\Delta$ ) is given by:

$$\Delta = \frac{A}{2k\epsilon_0} \left[ (V_{\mu\alpha} - \mu\beta)^2 + V^2\sigma_\alpha^2 + \sigma_\beta^2 - 2V \text{cov}_{(\alpha,\beta)} \right] \quad (1)$$

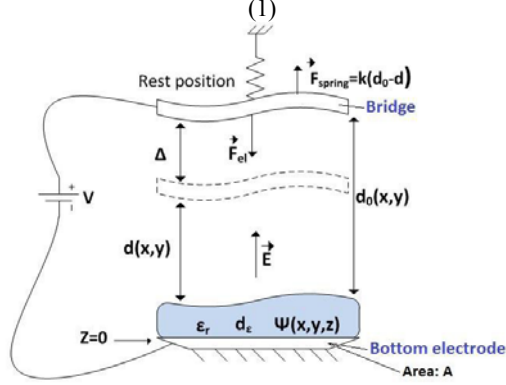


**Fig. 1.** Schematic model of a MEMS device with non-uniform trapped charge and air-gap distribution

where  $\mu$ ,  $\sigma^2$ , and  $\text{cov}$  are the mean, the variance and the covariance, respectively, of the capacitance per unit area  $[\alpha(x,y,\Delta)]$  and the induced charge density  $[\beta(x,y,\Delta)]$  at the armature area due to charges trapped at the dielectric. The relationships of  $\alpha(x,y,\Delta)$  and  $\beta(x,y,\Delta)$  are analytically given in [15].

According to the analysis in [18], for a small displacement of the moving electrode ( $\Delta \ll d_0(x,y)$ ) from the equilibrium position and neglecting the higher order terms, the capacitance per unit area distribution  $\alpha(x,y,\Delta)$  can be written as:

$$\alpha(x,y,\Delta) = \frac{\epsilon_0}{d_0(x,y) + \frac{d_\epsilon}{d_r}} \left[ 1 + \frac{\Delta}{d_0(x,y) + \frac{d_\epsilon}{d_r}} \right] = \alpha(x,y,0) + \alpha(x,y,0)^2 \cdot \frac{\Delta}{\epsilon_0} \quad (2)$$

The switch measured capacitance,  $C(V)$ , can be then calculated by integrating Eq.2 over the active area and the substitution of  $\Delta$  from Eq.1 leads to:

$$C(V) = A_{\mu\alpha} + \frac{A^2}{2k\epsilon_0^2} (\mu_\alpha^2 + \sigma_\alpha^2) \left[ (V_{\mu\alpha} - \mu\beta)^2 + V^2\sigma_\alpha^2 + \sigma_\beta^2 - 2V \text{cov}_{(\alpha,\beta)} \right] \quad (3)$$

where  $\mu_\alpha$  and  $\sigma_\alpha$  are the mean value and the variance of the capacitance per unit area, measured at applied bias  $V$ . The derivative of capacitance is thus given by:

$$\frac{dC(V)}{dV} = \frac{A^2}{k\epsilon_0^2} (\mu_\alpha^2 + \sigma_\alpha^2) \left[ (\mu_\alpha^2 + \sigma_\alpha^2)V - \mu_\alpha\mu_\beta - \text{cov}_{(\alpha\beta)} \right] \quad (4)$$

Eq.4 indicates that there is a linear dependence of MEMS up-state capacitance derivative on the applied voltage, with slope S and abscissa  $V_0$ :

$$S = \frac{A^2}{k\epsilon_0^2} (\mu_\alpha^2 + \sigma_\alpha^2)^2 \quad (5)$$

and

$$V_0 = \frac{\mu_\alpha\mu_\beta + \text{cov}(\alpha, \beta)}{\mu_\alpha^2 + \sigma_\alpha^2} \quad (6)$$

The above analysis clearly shows that in the general case of non-flat electrode switches the slope must be proportional to  $(\mu_\alpha^2 + \sigma_\alpha^2)$  and inverse proportional to the magnitude of spring constant k, when the displacement of the moving electrode from the equilibrium position is small. Thus the evolution of slope S, during a stress as well as a recovery test process, will provide valuable information on the deformation of the electrode, as long as the variance of the moving electrode remains practically constant for small displacements close to equilibrium. On the other hand, it may provide insight on the presence of a non-planarity that may give rise to uncontrolled stress gradient and the formation of a dipole across the dielectric film, due to contacted or field emission charging. In such a case, the up-state capacitance variance will significantly vary with applied bias leading to a non-linear derivative and hence non-constant S.

### 3. Experimental Details

The switches used in the present work are bridge-type capacitive switches fabricated with a standard photolithographic process on high resistivity silicon substrates on top of which a 3  $\mu\text{m}$   $\text{SiO}_2$  film was deposited. The silicon nitride ( $\text{SiN}_x$ ) dielectric film was grown on top of an electroplated gold (Au) layer with HF (13.56 MHz) PECVD method at 200 °C and the thickness of the film is 250 nm. XPS measurements revealed that the stoichiometry of the investigated silicon nitride ( $\text{SiN}_x$ ) films is  $x = \text{N/Si} \approx 1.04$ . The membrane consisted of an evaporated titanium (Ti) – gold (Au) seed layer followed by a gold (Au) electroplated layer

of 2.0  $\mu\text{m}$  thickness. A 2.2  $\mu\text{m}$  sacrificial layer was used to determine the up-state position of the bridge. The active area of the switches is  $2.5 \times 10^{-5} \text{ cm}^2$  and the pull-in voltage is  $V_{\text{pull-in}} = 20 \text{ V}$ .

The contacted charging was performed under a bias of 30 V and the up-state C-V characteristics were monitored after each successive stress step or after the end of stress process with the aid of a Boonton 72B capacitance meter with a resolution of 0.2 fF, while sweeping the voltage in 50 mV steps. The acquired bias was applied to the transmission line by a 6487 Keithley voltage source picoampere meter. The duration of each stress step was 30 s while the total stress time was 5 min. The discharging process was monitored for time length up to  $10^4$  s. Finally, all measurements have been performed under vacuum in a cryostat, with prior 2 hours annealing at 140  $^{\circ}\text{C}$  in order to minimize interference from humidity [3].

#### 4. Results and Discussion

The typical up-state C-V characteristic of a MEMS capacitive switch, according to Eq. 3, must exhibit a parabolic shape for small moving armature displacement from equilibrium state ( $\Delta \ll d_0$ ) and the shape of the parabola is expected to be determined by the device mechanical properties solely. Due to charging, the parabola will shift across bias axis with the magnitude of the shift determined by the net charge,  $\mu\beta$ , while the value of minimum capacitance may increase or decrease

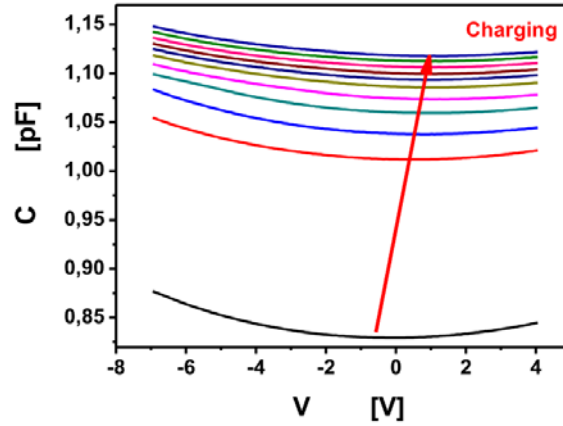
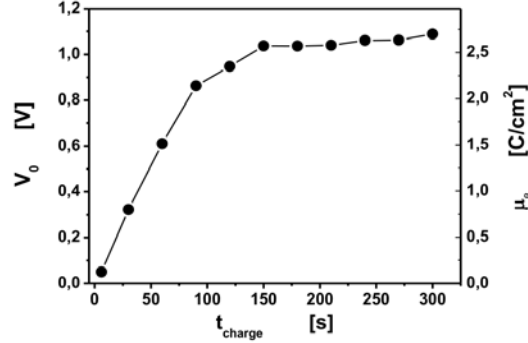


Fig. 2. (Color on line). Parabolic up-state C-V characteristics of a switch during charging.

with respect to the ideally uncharged film depending on both the charge distribution

variance and the mechanical properties degradation.



**Fig. 3.** The shift of bias  $V_0$  during charging and the corresponding values of equivalent surface charge density  $\mu\beta$  calculated assuming that we have a uniform charge distribution and that the switch electrodes are parallel.

Figure 2 shows the up-state parabolic C-V characteristics of a switch that exhibit a good agreement with the theoretical one, predicted by Eq. 3. The C-V characteristics shift to positive voltages after each successive stress step with a positive bias and the shift of bias  $V_0$  for capacitance minimum is presented in Fig. 3. Assuming that we have a uniform charge distribution ( $\sigma_2 = 0$ ) and that the switch electrode plates are parallel ( $\sigma_2 = 0$ ), which leads to zero covariance of parameters  $\alpha$  and  $\beta$  ( $\text{cov}_{\alpha,\beta} = 0$ ), we have also calculated the equivalent charge density  $\mu\beta$  from Eq. 6 after each successive stress step and the results are shown in the right axis of Fig.3.

The minimum capacitance is found to increase with stress (Fig. 2), a behavior that has been reported to arise from the increase of charge distribution variance [15]. Here it must be pointed out that according to the proposed model, taking into account Eq. 6, the capacitance minimum measured at  $V_0$  is given by:

$$C_{\min}(V_0) = A\mu_\alpha + \frac{A^2}{2k\epsilon_0^2} \left[ (\mu_\alpha^2 + \sigma_\alpha^2)(\mu_\beta^2 + \sigma_\beta^2) - (\mu_\alpha\mu_\beta + \text{cov}_{(\alpha,\beta)}) \right] \quad (7)$$

revealing a complex dependence on the parameters that are introduced to describe the deviation from the ideal case. The derivative of the C-V characteristics before and after two charging steps are plotted in Fig. 4a. In spite of the measurements' noise the derivative exhibit a linear relation with the applied voltage, as shown by applying linear fit to our experimental results. A fast decrease of the C-V characteristic's derivative slope  $S$  for the same switch as the charging process evolves with time is presented in Fig. 4b. Assuming a short stress time, we may attribute this behavior to uncontrolled stress gradient and to the formation of a non-uniform charge distribution, the scale of which may give rise to the formation of a dipole across the dielectric film. This behavior, according to Eq. 5, may affect

the nominator  $(\mu_\alpha^2 + \sigma_\alpha^2)$  and taking into account that the minimum capacitance

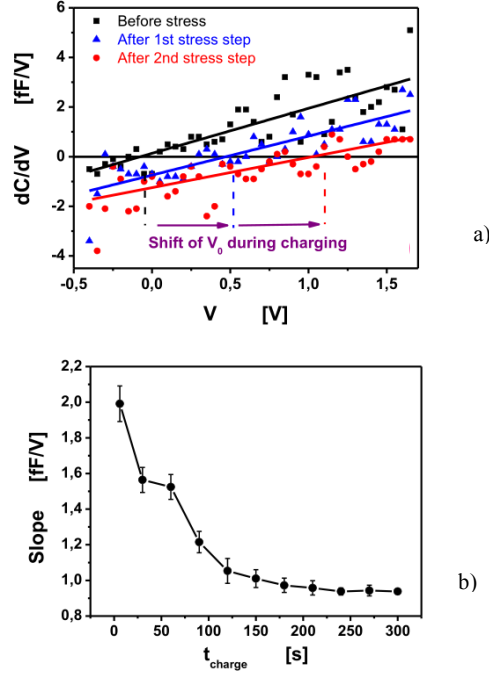


**Fig. 4.** (a) Typical capacitance derivatives before and after two stress steps and (b) the dependence of the slope  $S$  on the charging time.

increases with stress time (Fig. 2), we are led to the conclusion that the switch may exhibit a large capacitance variance  $\sigma_\alpha$  that decreases significantly during stress. We also mention that the decrease of  $S$  due to an increase of the spring constant  $k$  cannot be overruled, because stress induced hardening, *i.e.* increase of dynamic spring constant with stress time, has been observed in ultrafine crystalline nickel devices [19] and also alternating hardening and softening behavior has been reported until fracture in Au films [20].

The discharge process for the same switch has been also investigated by monitoring the shift of the up-state C-V characteristics during discharge and the previous theory model has been applied. The up-state C-V characteristics are parabolic and the minimum up-state capacitance decreases with time during discharge (Fig. 5a). Moreover, it has been found that the C-V characteristic's derivative slope  $S$  decreases with discharging time (Fig. 5b). This behavior is similar to the one observed during charging but the decrease rate is much lower. As already mentioned, the decrease of slope may result from a decrease of the nominator  $(\mu_\alpha^2 + \sigma_\alpha^2)$  (Eq. 5), which arises from the decrease of minimum

capacitance (Fig. 5a) and/or the decrease of  $\sigma_{\alpha}^2$  due to the charge draining by the bottom electrode and the redistribution across the surface of the dielectric film [11]. Finally, the gradual recovery of the mechanical properties cannot be ignored.

## 6. Conclusion

An analytical model for the up-state capacitance-voltage characteristic has been presented for the case of a real MEMS capacitive switch with non-uniform charge and capacitance distributions. The derivative of the C-V characteristic allows the separation of the parameters involving mechanical properties and electrical ones, that is the charging of the dielectric film. The application of the model to switches with smooth parabolic C-V characteristics revealed that the slope

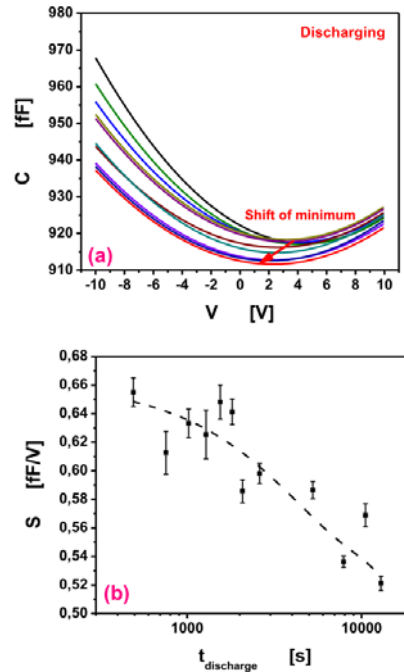


**Fig. 5.** (a) Up-state C-V characteristics of a switch during discharge and (b) the dependence of the slope S on the discharging time (dashed line shows the trend of our data).

of the C-V characteristic derivative decreases with stress time suggesting a decrease of capacitance variance or rather an increase of spring constant, the latter being presently under further investigation. The slope of the C-V characteristic



derivative has been also found to decrease during discharge, but the decrease in this case is much lower. Finally, considering all these, we conclude that the slope of the C-V characteristic's derivative in MEMS capacitive switches requires further investigation in order to extract the important information on the device degradation.

**Acknowledgements.** The first author, Matroni Koutsourelis, would like to thank *IKY Fellowships of Excellence for Postgraduate Studies in Greece – Siemens Program* that takes place in the framework of the Hellenic Republic – Siemens Settlement Agreement.

## References

- [1] G.M. REBEIZ, *RF MEMS theory, design and technology* Hoboken, Wiley, New Jersey, USA (2003) 185-215.
- [2] G. PAPAIOANNOU, *Dielectric Charging in Advance F MEMS* E. S. Lucyszyn, Cambridge University Press (2010) 140-187.
- [3] G. PAPAIOANNOU and R. PLANA, *Physics of Charging in Dielectrics and Reliability of Capacitive RF-MEMS Switches* in *Advanced Microwave and Millimeter Wave Technologies Semiconductor Devices Circuits and Systems*, Ed. M. Mukherjee (2010) 275-301.
- [4] C. GOLDSMITH, J. EHMKE, A. MALCZEWSKI, B. PILLANS, S. ESHELMAN, Z. YAO, J. BRANK AND M. EBERLY, *Lifetime characterization of capacitive RF MEMS switches*, IEEE MTT-S International Microwave Symposium Digest. **1** (2001) 227 – 230.
- [5] W.M. VAN SPENGEN, R. PUERS, R. MERTENS AND I. DE WOLF, *A comprehensive model to predict the charging and reliability of capacitive RF MEMS switches*, J. Micromech. Microeng. **14**, (2004) 514-521.
- [6] C.L. GOLDSMITH, D.I. FOREHAND, Z. PENG, J.C.M. HWANG AND J.L. EBEL, *High-cycle life testing of RF MEMS switches*, IEEE International Microwave Symposium (MTT-S) (2007), 1805 – 1808.
- [7] P. CZARNECKI, X. ROTTENBERG, P. SOUSSAN, P. EKKELS, P. MULLER, P. NOLMANS, W. DE RAEDT, H.A.C. TILMANS, R. PUERS, L. MARCHAND AND I. DE WOLF, *Effect of substrate charging on the reliability of capacitive RF MEMS switches*, Sensors and Actuators A (2009) 261–268.
- [8] J. WIBBELER, G. PFEIFER, M. HIETSCHOLD, *Parasitic charging of dielectric surfaces in capacitive microelectromechanical systems (MEMS)*, Sensors and Actuators A (1998) 74-80.
- [9] R.W. HERFST, H.G.A. HUIZING, P.G. STEENEKEN and J. SCHMITZ, *Characterization of dielectric charging in RF MEMS capacitive switches*, in Proc. IEEE Int. Conf. on Microel. Test Struct. (ICMTS) (2006) 133-136.
- [10] R.W. HERFST, P.G. STEENEKEN and J. SCHMITZ, *Time and voltage dependence of dielectric charging in RF MEMS capacitive switches*, in Proc. IEEE 45<sup>th</sup> Annual International Reliability Physics Symposium (IRPS) (2007) 417-421.
- [11] R.W. HERFST, P.G. STEENEKEN, H.G.A. HUIZING and J. SCHMITZ, *Center-shift method for the characterization of dielectric charging in RF MEMS capacitive switches*, IEEE Trans. on Semiconductor Manufacturing **21** (2008) 148-153.
- [12] G. PAPAIOANNOU, J. PAPAPOLYMEROU, P. PONS and R. PLANA, *Dielectric charging in radio frequency microelectromechanical system capacitive switches: A study of material PROPERTIES AND DEVICE PERFORMANCE*, Applied Physics Letters **90** (2007).
- [14] S. KIM, S. CUNNINGHAM and A. MORRIS, *Characterization of dielectric charging and reliability in capacitive RF MEMS switches*, in Proc. IEEE Int. Reliab. Phys. Symp. (IRPS) (2013) 6B.4.1 - 6B.4.5.
- [15] X. ROTTENBERG, I. DE WOLF, B.K.J.C. NAUWELAERS, W. DE RAEDT and H.A.C.

- TILLMANS, *Analytical model of the DC actuation of electrostatic MEMS devices with distributed dielectric charging and nonplanar electrodes*, J. of Microelectromech. Syst. 16 (2007) 1243-1253.
- [16] M. KOUTSOURELI and G. PAPAIOANNOU, *Determination of long time discharge current in microelectromechanical system capacitive switches*, Appl. Phys. Lett. **99** (2011).
- [17] M. KOUTSOURELI, L. MICHALAS, P. MARTINS, E. PAPANDREOU, A. LEULIET, S. BANSROPUN, G. PAPAIOANNOU and A. ZIAEL., *Microel. Reliab.* **53** (2013).
- [18] D. BIRMPILIOTIS, P. CZARNECKI, M. KOUTSOURELI, G. PAPAIOANNOU and I. DE WOLF, *Assessment of dielectric charging in capacitive MEMS switches fabricated on Si substrate with thin oxide film*, Microelectronic Engineering **159** (2016) 209–214.
- [19] HSU H.H. and D. PEROULIS, *A viscoelastic-aware experimentally-derived model for analog RF MEMS varactors*, IEEE 23<sup>rd</sup> Int. Conf. on Micro Electro Mechanical Systems (MEMS) (2010) 783 – 786.
- [20] I. CHASIOTIS, C. BATESON, K. TIMPANO, A.S. MCCARTY, N.S. BARKER and J.R. STANEC, *Strain rate effects on the mechanical behavior of nanocrystalline Au films*, Thin Solid Films, **515** (2007) 3183–3189.